Synthesis and Physico-Chemical Study of Epoxy-Maleate of 9,9'-Bis(4-hydroxyphenyl)anthrone-10 and its Jute and Glass Composites

JABAL D. THANKI, JIGNESH P. PATEL AND PARSOTAM H. PARSANIA*

Polymer Chemistry Division, Department of Chemistry, Saurashtra University, Rajkot-360 005, Gujarat, India

ABSTRACT

Epoxy maleate of 9,9'-bis(4-hydroxyphenyl)anthrone-10 (EANM) was synthesized and its jute (J-EANMS) and glass(G-EANMS) composites were prepared by hand layup compression molding technique under 20 bar at 120°C for 5h. The structure of EANM was supported by FTIR and ^{1}HNMR spectroscopic techniques and also characterized by acid and hydroxyl values. Thermal properties of EANM and cured EANMS were evaluated by DSC and TGA at 10°C min^{-1} heating rate in nitrogen atmosphere. EANM and EANMS are thermally stable up to 149^{o} and 300°C and followed three and single step degradation kinetics. The energy of activation, frequency factor, degradation order and entropy change were evaluated and compared. J-EANMS and G-EANMS showed 38.2 and 184MPa tensile strength; 31.6 and 90.3 MPa flexural strength, 4.4 and 5.7 kVmm^{-1} electric strength and 2.6x10^{12} and 4.2x10^{12} ohm cm volume resistivity, respectively. Good thermo-mechanical and electrical properties and excellent hydrolytic stability against different environments indicated its industrial utility as low load bearing housing, insulating material for electrical and electronic appliances and marine applications.

KEYWORDS : *Epoxy, FT-IR, NMR, DSC, TGA, Mechanical and Electrical properties, Composites, Activation energy, Degradation*

INTRODUCTION

Vinyl ester resins are prime thermosetting materials with excellent physico-chemical properties are the most suitable for manufacturing of reinforced pipes, tanks, scrubbers, marine crafts [1]. They also useful for coatings, adhesives, molding compounds, structural laminates, and electrical

J. Polym. Mater. Vol. **35,** No. 2, 2018, 231-243

Correspondence author e-mail: phparsania22@gmail.com, phparsania@goi.com

applications[2] . Generally tertiary amines, pyridine, triphenyl phosphine, imidazole, phosphine, alkali, etc. are used as catalysts for the synthesis of vinyl ester resins[3,4] . Most commonly styrene is used as a reactive diluent and free radical generating initiators[5,6]. Commonly methyl ethyl ketone peroxide is used as an initiator along with suitable promoters. Cured vinyl ester resins possess excellent thermo-mechanical, electrical and chemical resistance make them suitable for several industrial applications.

Recently several investigators have reported the synthesis, curing, fabrication of filled and unfilled fiber reinforced composites and carried out their spectral, thermal mechanical, electrical, water absorption, etc. studies[7-18] . They observed very good to excellent studied physico-chemical properties for various industrial applications. The selection of the materials for various industrial applications is mainly based on thermo-mechanical, electrical and chemical resistance properties of the materials. Fiber-matrix interfacial adhesion, degree of resin cure, impurities, humidity, temperature, nature of polymers and fillers, additives, extent of ageing, electrode material, electrode area, sample thickness, voltage application time, current frequency, etc. affect the electrical properties of the polymeric composites[19] .

To the best of our knowledge no work has been reported in the literature on epoxy maleate of 9,9'-bis(4-hydroxyphenyl)anthrone-10, which encouraged us to investigate present work. In this work we have synthesized epoxy maleate of 9,9'-bis(4-hydroxyphenyl)anthrone-10 (I) and

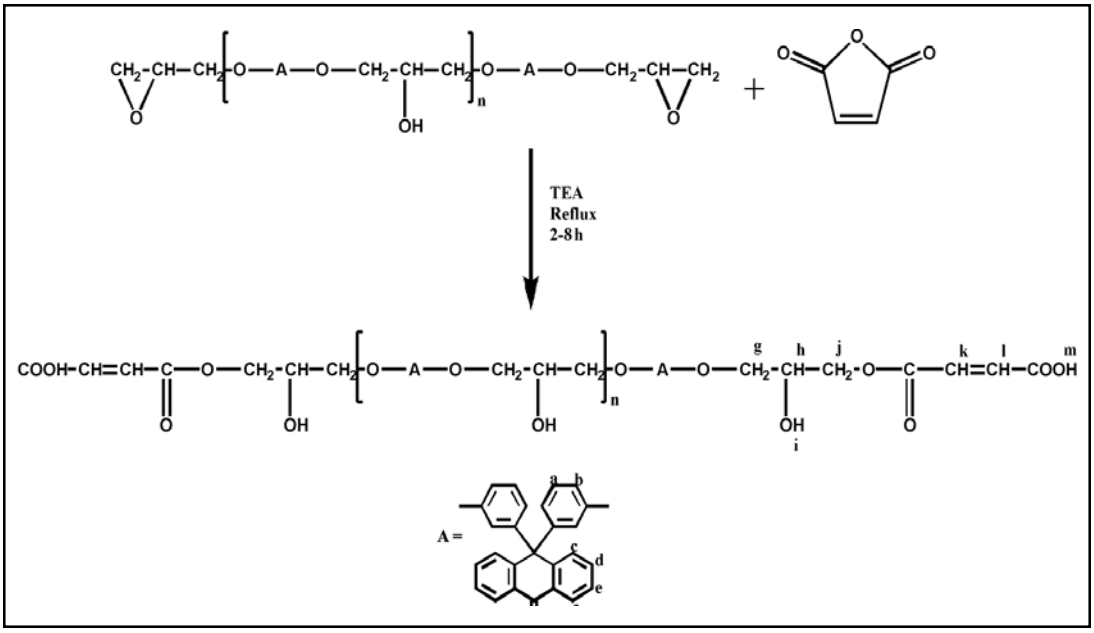

characterized by acid and hydroxyl values, spectral and thermal techniques. Using styrene as a reactive diluent, jute and glass composites are prepared and evaluated their mechanical and electrical properties and chemical resistance against water, acids, alkalis and salt.

EXPERIMENTAL

Materials and Methods

Solvents and chemicals used in the present work were of laboratory grade and used as received or purified according to reported methods[20]. Epoxy resin of 9,9'-bis(4-hydroxyphenyl)anthrone-10 (EAN, EEW 940) was synthesized and purified according to our recent reported work[21]. Silane treated E-glass fabric (7mil) and woven jute fabric (Brown jute, Corchorus capsularis) were purchased from Unnati Chemicals, Ahmedabad and from local market, respectively.

Synthesis of Epoxy Maleate of 9,9'-Bis(4-hydroxyphenyl)anthrone-10

Epoxy maleate of 9,9'-bis(4-hydroxyphenyl)anthrone-10 (Scheme 1) here after designated as EANM, was synthesized as follows. Into a 500 mL three-neck flask 0.1 eq (94.2 g) of EAN was dissolved in 250 mL acetone. To this solution 0.22 mol maleic anhydride, 10 mL xylene and 1 mL triethylamine catalyst were added with stirring. The temperature of the resultant solution was brought to reflux. The samples were withdrawn at the interval of 1h starting from 2h onwards. The water formed during the reaction was separated as an azeotropic mixture by Dean and Stark apparatus. The reaction mass was cooled to room temperature and brownish red colored resin was isolated from water, filtered, washed well with hot distilled water and finally with cold methanol and dried at room temperature. The resin was found soluble in common organic solvents. Resin was purified three times from MEK-water system prior to its use.

Preparation of Jute and Glass Composites of Epoxy Maleate

Required quantity of EANM and styrene (Table 1) were transferred into a 500 mL beaker containing 100 mL tetrahydrofuran and stirred well at room temperature. To this solution 2% methylethylketoneperoxide and 1% of 6%-cobalt naphthenate of mixed matrix material were added as an initiator and as an accelerator, respectively. Resultant solution was stirred well and was applied to jute (350 GSM) / glass (450 GSM) fabrics (24 cm × 24 cm) with a smooth brush and solvent was allowed to evaporate at room temperature. Eight jute and ten glass impregnated fabrics were stacked one over the other between two mylar films. The stacked plies were kept between two teflon sheets. These teflon sheets were kept between two preheated stainless steel plates and pressed under 20 bar pressure at 120°C for 5h and 2h at room temperature. Silicone spray was used as a mold releasing agent. Here after jute and glass composites are designated as J-EANMS and G-EANMS, respectively. Samples with required dimensions were machined for tensile and flexural tests.

TABLE 1. Mechanical and electrical properties of J-EANMS and G-EANMS

Parameter	J-EANMS	G-EANMS
Jute/Glass fabric, g	180	110
EANMS, g	90	55
Styrene, g	90	55
Tensile strength, MPa	38.2	184
Flexural strength, MPa	31.6	90.3
Electric strength, $kVmm^{-1}$	4.4	5.7
Volume resistivity, ohm cm	$2.6x10^{12}$	$4.2x10^{12}$

For chemical resistance test samples of 3 cm x 3 cm were machined and edges were sealed with matrix material.

Measurements

Acid and hydroxyl values of EANM were determined according to standard methods[22, 23]. The FTIR spectrum of EANM was scanned on a Shimadzu 1S-IR affinity FTIR spectrometer over the frequency range from 4000-600 cm^{-1}. The ^{1}HNMR spectrum of EANM was scanned on a Bruker AVANCE II (400MHz) spectrometer by using DMSO-d6 as a solvent and TMS as an internal standard. Differential Scanning Calorimetric (DSC) and Thermo Gravimetric (TG) thermograms of EANM and EANMS were scanned on a Shimadzu DSC-60 and Shimadzu DTG-60H, respectively at 10°C min^{-1} heating rate in nitrogen atmosphere (flow rate 100 mL min^{-1}) using standard aluminum pans. Known mass of the samples were taken in aluminum pans covered by empty aluminum lids and sealed using a crimper. The DSC and TG thermograms were scanned over the temperature range from 40-350°C and 40-700°C, respectively. Tensile (ASTM D 638-01) and flexural (ASTM D-790-03) strengths of J-EANMS and G-EANMS were measured on a Shimadzu Autograph Universal Tensile Testing Machine, Model No. AG-X Series at a speed of 10 $mmmin^{-1}$. Electric strength (IEC-60243-Pt-1-1998) and volume resistivity (ASTM-D-257-2007) measurements were made on a high voltage tester (Automatic Electric-Mumbai) in air at 27°C by using 25/75mm brass electrodes and a Hewlett Packard high resistance meter in air at 25°C after charging for 60 sec at 500 V DC applied voltage at ERDA Vadodara, Gujarat. Replicate measurements (3-5) on each sample were performed and average values were considered. Water absorption study was carried out at room temperature (30 ± 2°C) according to ASTM D570-98 by a change in mass method against distilled water, 10% NaCl, 10% HCl, 10% HNO_3, 10% H_2SO_4, 10% NaOH, and 10% KOH. Preweighed samples were immersed in distilled water, 10% NaCl, 10% HCl, 10% HNO_3, 10% H_2SO_4, 10% NaOH, and 10% KOH solutions at room temperature. Samples were periodically taken out from the solutions, wiped surfaces with tissue papers on both the sides, reweighed and reimmersed in the solutions. The process was carried out till equilibrium was established.

RESULTS AND DISCUSSION

Acid and Hydroxyl Values

Acid and hydroxyl values of EANM at different interval were determined volumetrically. Average of three measurements on each of the samples with time is reported in Table 2 from which it is observed that acid value decreased and hydroxyl value increased with reaction time confirming almost conversion of epoxide groups into ester groups.

Spectral Analysis

FTIR spectrum of EANM is presented in Fig. 1 and characteristic IR absorption frequencies (cm^{-1}) are 3417.8 and 3277.8 (O-H, str.), 2954.7 (C-H, asym. str.), 1662.8 (ester and ketone C=O, str.), 1568.9 (C=C, str.), 1422.8 (Alkane C-H, def.), 1230.3 (Ar-O-R, str.), 1027 (C-H, ipd and C-OH def.), 860.4 (C-H, oopd.) and 708.9 (C-H, oopd). ^{1}HNMR (DMSO-d6) spectrum of EANM is presented in Fig. 2 from which it is observed that the spectrum is complex. Different types of protons and their chemical shifts (ppm) are assigned as follows: 2.86 [d, -OCH_2, (g)], 2.93 [d, -CH_2O, (j)], 3.57

TABLE 2. Acid and hydroxyl values of EANM.

Time, h	2	3	4	5	6	7	8
Acid value, mg KOH/g	24.7	18.2	12.9	10.7	8.2	6.5	4.3
Hydroxyl value, mg KOH/g	84.2	171.6	268.2	341.5	463.2	514.9	587.2

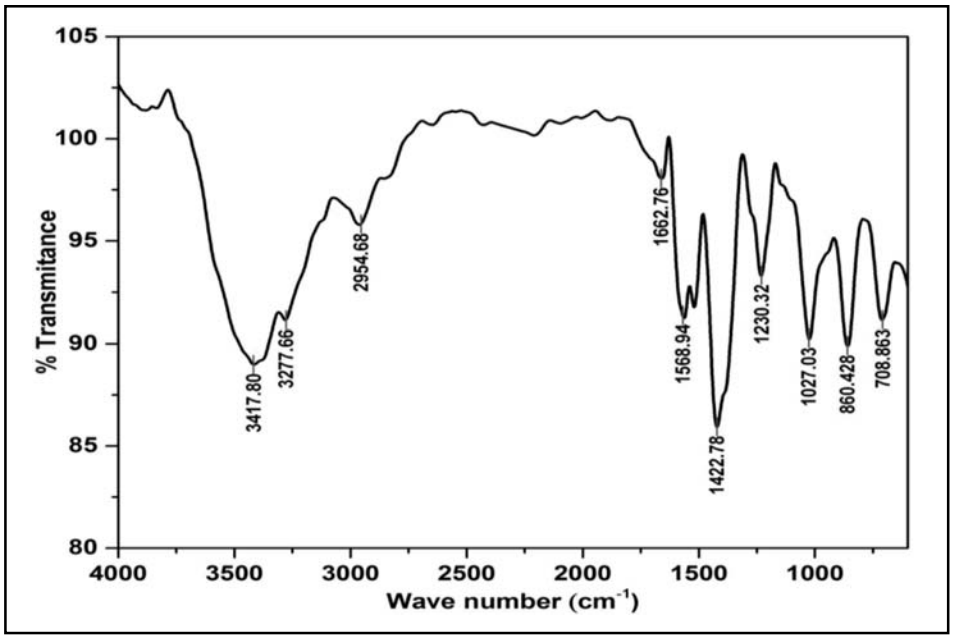

Fig. 1. FTIR spectrum of epoxy maleate of 9, 9'-bis (4-hydroxyphenyl) anthrone-10 (EANM).

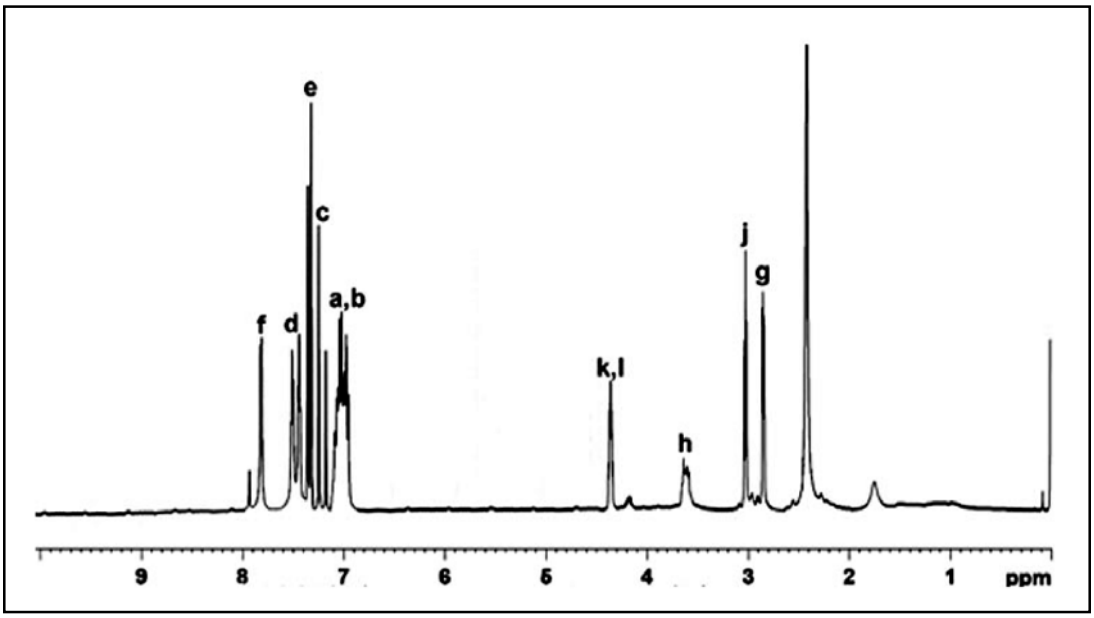

Fig. 2. ^{1}HNMR(400MHz) spectrum of epoxy maleate of 9,9'-bis(4-hydroxyphenyl)anthrone-10 (EANM) in DMSO-d6.

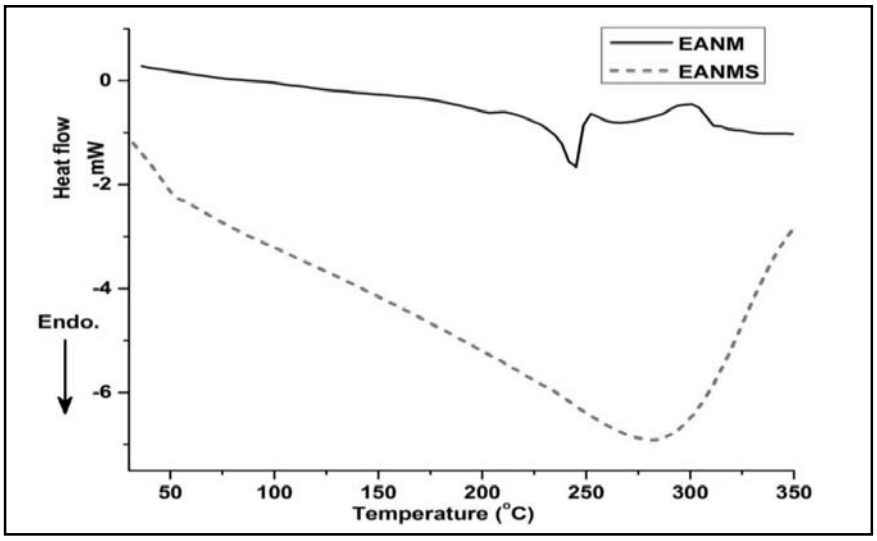

Fig. 3. DSC curves of EANM and EANMS at 10°C min^{-1} heating rate in nitrogen atmosphere

[m, -CH(OH) (h)], 4.30 [s, —OH(i)],7.05 [m, -ArH, (a, b, k, l)], 7.11 [d, -ArH, (c)], 7.29 [d, -ArH, (e)], 7.40 [d, -ArH, (d)], 7.81 [d, -ArH, (f)] and 7.9[s, -COOH(m). Residual DMSO and moisture appeared at about 2.50 and 4.2, respectively. Thus, IR and NMR data supported the structure of EANM.

Thermal Analysis

DSC thermograms of EANM and EANMS at 10°C min^{-1} heating rate in nitrogen atmosphere are presented in Fig.3. EANM showed endothermic transition at 243.84°C and exothermic transition at 301.91°C due to thermal polymerization followed by decomposition reactions and further confirmed by weight loss over that temperatures in its TG thermogram (Fig. 4). EANMS showed a broad endothermic transition centered at 281.94°C due to some physical change and confirmed by no weight loss at this temperature in its TG thermogram.

From Fig. 4, it is clear that EANM is thermally stable up to about 149°C and followed three-step degradation reactions, while EANMS is thermally stable up to about 300°C and followed single step degradation reaction. EANMS showed excellent thermal stability than EANM is due to high degree of cross linking density. EANM showed 6.1% weight loss over temperature range from 149 °C to 227°C may be due to decarboxylation followed by thermal polymerization of terminal acid groups. Initial decomposition temperature (T_o), decomposition range, temperature of maximum weight loss (T_{max}), % weight loss, and % residue remained at 700°C for EANM and EANMS are presented in Table 3. T_{max} values were derived from dw/dt against Temperature plots.

Associated kinetic parameters such as energy of activation (E_a), frequency factor (A) and order of the reaction (n) for both the samples were derived according to Anderson-Freeman method [24]:

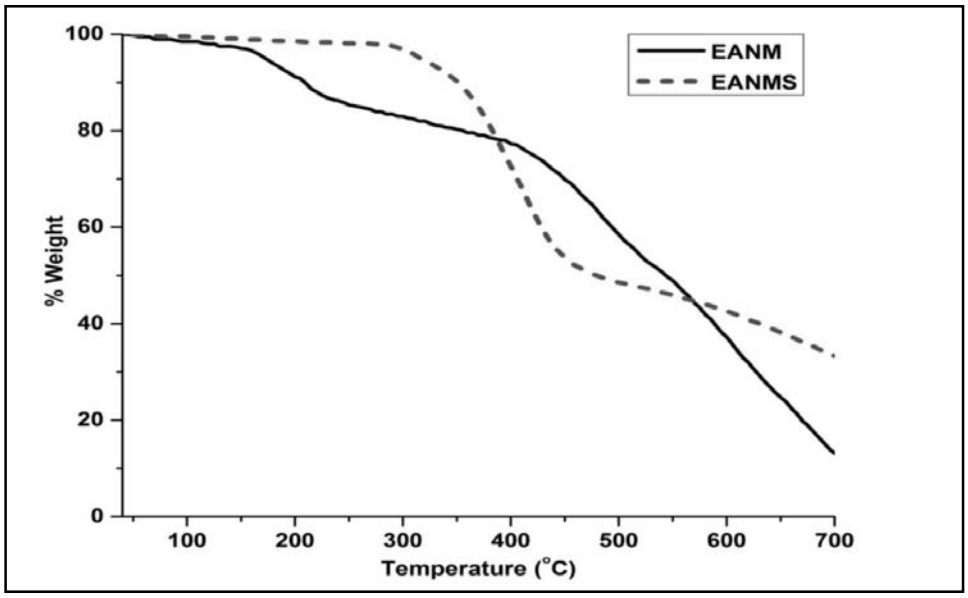

Fig. 4. TGA thermograms of EANM and EANMS at 10°C min^{-1} heating rate in nitrogen atmosphere.

TABLE 3. TGA data of EANM and EANMS.

Sample	T_o, °C	Decompn. range, °C	T_{max}, °C	% Wt loss	% Residue at at 700 °C
EANM	149	149-227	181.4	6.1	15.1
		245-352	306.6	29.6	
		496-628	553.3	18.2	
EANMS	300	300-502	402.5	49.3	33.5

$$\Delta ln\frac{dw}{dt} = n\Delta W - \left(\frac{E_a}{R}\right)\Delta\left(\frac{1}{T}\right) \quad (1)$$

$$A = \frac{E_a\beta}{RT^2}\, e^{E_a/RT} \quad (2)$$

$$\Delta S^* = \mathrm{R}\ln\frac{\mathrm{Ah}}{\mathrm{kT}} \quad (3)$$

Where dw/dt is the rate of decomposition, W is the active mass, β is the heating rate, R is the gas constant, h is the Planck's constant, T is temperature and k is the Boltzmann constant. The entropy change ΔS* was determined at corresponding Tmax.The least square values of above mentioned parameters along with regression coefficients (R^2) are reported in Table 4. First and third step degradation reactions of EANM followed apparently first order degradation kinetics, while second step followed second order kinetics. The E_a values of first and second steps are comparable and much smaller than that of second step probably due to very rigid nature of thermally cross-linked EANM. The ΔS*

TABLE 4. Kinetic parameters of EANM and EANMS.

Sample	Ea, kJmol $^{-1}$	A, s $^{-1}$	ΔS * , JK mol $^{-1}$	n	R^2
EANM	67.11	3.36 x 10^5	-142.63	1.39	0.9881
	197.21	6.93 x 10^{15}	52.81	2.27	0.9966
	72.61	82.8	-216.67	0.88	0.9970
EANMS	77.82	3.55x10^3	-183.76	1.12	0.9952

values of first and second steps are negative and large in magnitudes, while for second step it is positive and relatively large in magnitude. The E_a value of EANMS is somewhat higher than those of first and second step degradation reactions of EANM but much smaller than that of second step degradation reaction due to much rigid nature of thermally cross-linked EANM. Low value of E_a of EANMS may be accounted for flexible polystyrene bridges. EANMS also followed apparently first order degradation kinetics. Negative and large magnitudes of ΔS* indicated that the transition states are in orderly states than initial states and vice versa [25, 26].

Degradation reactions are complex reactions and involve a variety of reactions. Ether, ester and side substituents in the cross-linked resins are thermally weak linkages and preferentially degradation starts from such weak points in accordance to bond strength and lead to formation of free radicals, which further undergo a variety of reactions with evolution of hydrocarbon gases. Relatively large residues (15-34%) at 700°C confirmed formation of highly thermally stable cross-linked products. Thus, EANMS showed excellent thermal stability with large residue at 700 °C signifying its importance as high performance polymer.

Mechanical and Electrical Properties

Tensile strength, flexural strength, electric strength and volume resistivity of J-EANMS and G-EANMS are presented in Table 1. It is observed that both the composites showed good tensile and flexural strengths. Both the composites showed moderately good electric strength, which indicated that composites are not sustainable to high voltages but they displayed good volume resistivity due to partial cancellation of dipolar charges present both in fiber and matrix. Both J-EANMS and G-EANMS showed comparable tensile strength and flexural strength with epoxy methacrylate of 9,9'-bis(4-hydroxyphenyl)anthrone-10-jute (J-EANMAS:38.8MPa tensile strength, 30.9 MPa flexural strength) and glass and (G-EANMAS:192.9 MPa tensile strength, and 90.1 MPa flexural strength) composites[21]. J-EANMS showed somewhat better electric strength than that of J-EANMAS (3 kVmm^{-1}), while G-EANMAS (5.9kVmm^{-1}) showed comparable electric strength. J-EANMS showed 14 times better volume resistivity than that of J-EANMAS (1.9x10^{11} ohm cm), while G-EANMA (3.1x10^{13} ohm cm) showed 7 times lower volume resistivity due to structural dissimilarity of both the matrices. Moderate to good mechanical and electrical properties of both the composites signified their industrial

importance for low load bearing housing and insulating applications.

Chemical Resistance

The interaction of chemicals with fiber reinforced composites proceeds through different mechanisms namely chemical reaction, solvation, absorption, plasticization and stress cracking and affects physical properties adversely. The chemical resistance of the composites depends upon bond strength, time, temperature, crystallinity, branching, polarity, concentration and reactivity of the reagents, etc.

Water absorption in composites is Fickian as well as non-Fickian in character [27, 28]. Assuming one dimensional diffusion in the composites, water absorption in J-EANMS and G-EANMS in different environments namely water, 10% each of aqueous NaCl, HCl, HNO_3, H_2SO_4, NaOH, and KOH was carried out at 30°C. The percentage water absorbed by the composites with the passage of time in a given environment at 30°C was determined according to Eqn. 4:

$$M_t = \frac{W_m - W_d}{W_d} X\ 100 \qquad (4)$$

Where M_t = % water absorbed at time t, W_m = weight of moist sample and W_d = weight of dry sample. The plots of % water absorbed against time for J-EANMS and G-EANMS are presented in Figs. 5 and 6, respectively. Equilibrium time and equilibrium water absorbed by J-EANMS and G-EANMS in different environments are presented in

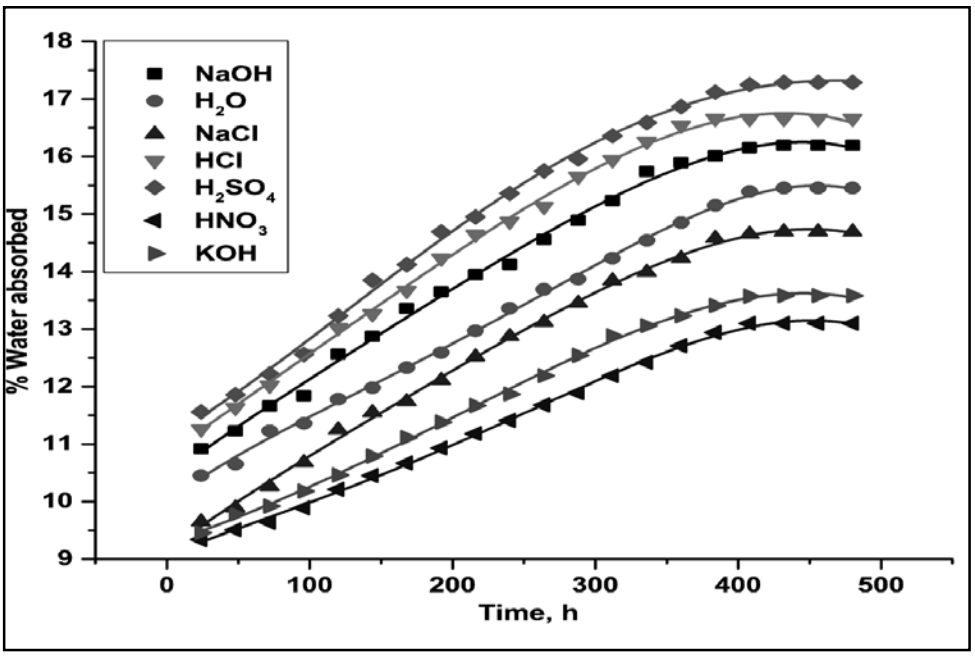

Fig. 5. The plots of % water absorbed against time for J-EANMS in 10% aq. each of NaCl, HCl, HNO_3, H_2SO_4, NaOH, KOH and distilled water at 30 °C.

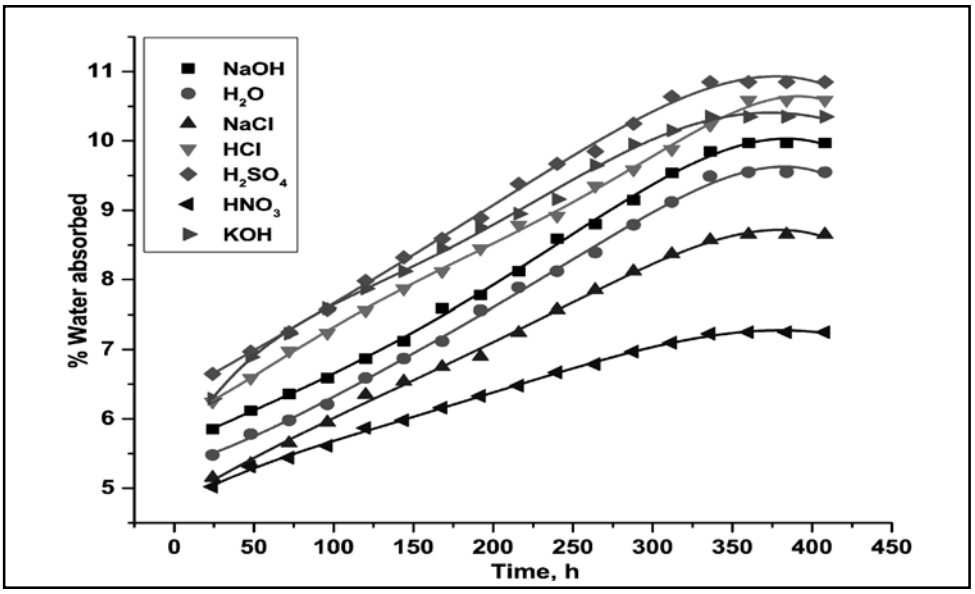

Fig. 6. The plots of % water absorbed against time for G-EANMS in 10% aq. each of NaCl, HCl, HNO_3, H_2SO_4, NaOH, KOH and distilled water at 30 °C.

Table 5. J-EANMS and G-EANMS showed 13.1-17.3% and 7.3-10.9% equilibrium water absorption tendency and 360-408h and 312-336h equilibrium time in 10% aq. each of NaCl, HCl, HNO_3, H_2SO_4, NaOH, KOH and distilled water at 30°C. Equilibrium time of G-EANMS is found somewhat shorter than that of J-EANMS due to different nature of both the composites. Observed % water absorption trends for J-EANMS and G-EANMS in different environments are H_2SO_4 > HCl > NaOH > H_2O > NaCl > KOH > HNO_3 and H_2SO_4 >HCl > KOH > NaOH > H_2O > NaCl > HNO_3, respectively. From Table 5, it is observed that the nature of electrolytes affected water structure and hence water absorption due to solvation phenomenon. The hydroxyl groups of matrix and jute fibers (cellulose, hemicellulose and lignin) are mainly responsible for high water absorption tendency in the composites. The nature of strong electrolytes affected the water structure and hence diffusivity in the composites. We have observed the effect of strong electrolytes on water absorption and diffusivity in our recent published work [25, 26].

Diffusivity in different environments was determined according to Eqns 5 and 6 by determining the initial slopes of the plots of % water absorption against $\sqrt{t}$:

$$M = \frac{4M_m}{h}\sqrt{\frac{t}{\pi}}\sqrt{\overline{D_x}} \quad (5)$$

$$D_x = \pi\left(\frac{h}{4M_m}\right)^2 (slope)^2 \quad (6)$$

Where M_m = % Equilibrium water absorption, D_x = Diffusivity and h=Sample thickness. Diffusivity in different environments for both composites is reported in Table 5. Observed

TABLE 5. Water uptake and diffusivity data of J-EANMS and G-EANMS at 30°C and in boiling water

Environment	Equilibrium time, h	Equilibrium water content	Diffusivity, D_x, 10^{-13}, $m^2 s^{-1}$	% Equilibrium water content in boiling water
		J-EANMS		
H_2O	408	15.5	1.57	15.2
HCl	360	16.7	2.70	
HNO_3	384	13.1	2.73	
H_2SO_4	408	17.3	3.47	
NaOH	408	16.2	2.45	
KOH	384	13.6	2.14	
NaCl	408	14.7	2.46	
		G-EANMS		
H_2O	336	9.6	3.51	8.2
HCl	336	10.6	3.29	
HNO_3	312	7.3	3.95	
H_2SO_4	312	10.9	3.96	
NaOH	336	10.0	1.87	
KOH	312	10.4	2.59	
NaCl	336	8.7	4.04	

diffusivity trends for J-EANMS and G-EANMS are $H_2SO_4 > HNO_3 \cong HCl > NaOH \cong NaCl > KOH > H_2O$ and $NaCl \cong H_2SO_4 \cong HNO_3 > H_2O > HCl > KOH > NaOH$, respectively. Thus the nature of strong electrolytes affected diffusivity in the composites without any damage. Absorption of water in the composites causes swelling of fibers till the cell walls are saturated with water and then after water exists as free water in the void structure leading to composites delamination or void formation. Fiber-matrix interfacial bonding is weaken by absorbed water and leads to hydrolytic degradation and thereby tensile property deteriorates slowly [29, 30]. Cracks and blistering of fibers lead to high water absorption in the composites [29, 30] .

Water Absorption in Boiling Water

The % water absorption in J-EANMS and G-EANMS was also carried out in boiling water. The % water absorbed by the composites with the passage of time is presented in Fig. 7. Equilibrium time and equilibrium water absorption for J-EANMS and G-EANMS are 10 and 9h; and 15.2 and 8.5%, respectively. In case of J-EANMS equilibrium time is reduced to 41 times, while in G-EANMS it is reduced to 37 times. Thus increasing temperature led to drastic reduction in equilibrium time without

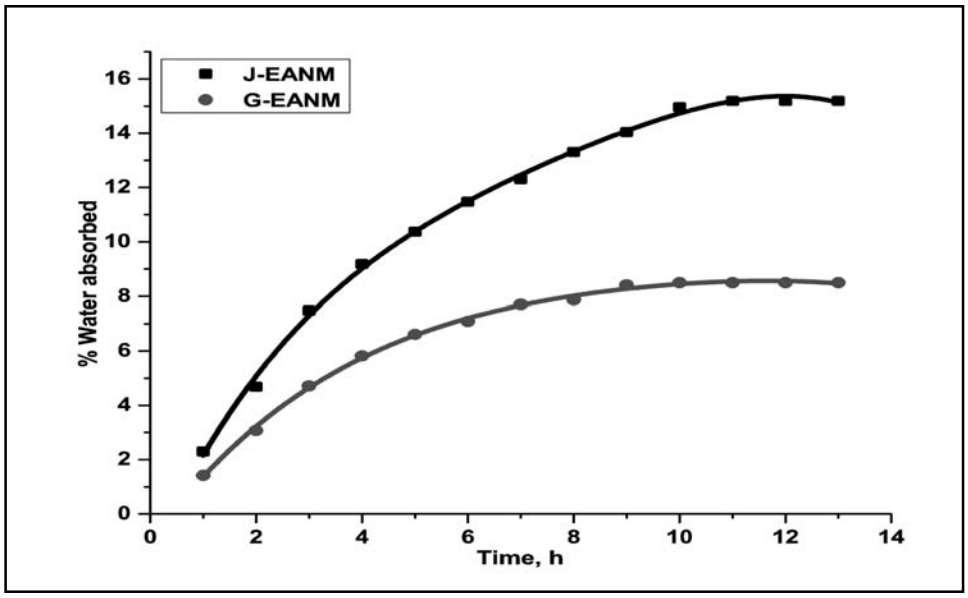

Fig. 7. The plots of % water absorbed against time for J-EANMS and G-EANMS in boiling water.

any damage. Thus, both the composites showed excellent hydrolytic stability in different environmental conditions indicating their marine applications.

CONCLUSIONS

Epoxy maleate of 9,9'-bis(4-hydroxyphenyl) anthrone-10 was synthesized and characterized by acid and hydroxyl values, spectral and thermal techniques. EANMS showed excellent thermal stability. Jute and glass composites showed good tensile and flexural strengths, moderate electric strength and good volume resistivity. Both the composites showed excellent hydrolytic stability in different environment. The electrolytic solutions affected water absorption and diffusivity in the composites. Both the composites may find their applications in housing and electrical fields.

ACKNOWLEDGEMENTS

The authors are thankful to FIST-DST and SAP-UGC for their generous financial support. Jabal Thanki is also thankful to University Grants Commission New Delhi for Junior Research Fellowship, Major Research Project Grants Sanction No. 42-246/2013.

REFERENCES

1. G. Marsh, *Reinf Plast,* 51(2007) 20
2. M. Sultania, S. B. Yadaw, J. S. P. Rai and D. Srivastava, *Mater. Sci. Eng.* A 27(2010) 4560.
3. B. K. Fink, T. A. Bogetti, M. A. Stone and J. W. Gillespie, *Army Research Laboratory* (*2002) 5-24.*
4. G. H. Hamedani, M. Ebrahimi and S. R. Ghaffarian, Ira. *Polym. J.* 15 (2006) 8*71-878.*
5. *B.* Lubin, Handbook of Composites, Van Nostrand Reinhold, New York. 1984.

6. C. A. Ma and M. Dekker, *Epoxy resin chemistry and technology,* New York, 1988.
7. E. Taylan and S. H. Kusefoglu, *J. Appl. Polym. Sci.* 112 (2009) 1184-1191.
8. M. Worzakowska, *J. Therm. Anal. Calorim.* 102 (2010)745-750.
9. P. K. Mer and P. H. Parsania, *Polym. Plast. Technol. Eng.* 50 (2011) 282-287.
10. M. M. Reboredo, M. I. Aranguren, and N. E. Marcovich, *J. Appl. Polym. Sci.* 61 (1996) 119-124.
11. L. Musa, A. Abubakar and H. D. Rozman, *Polym. Plast. Technol. Eng.* 44 (2005) 489-500.
12. A. Hazlan, A. Abubakar and H. D. Rozman, *Polym. Plast. Technol. Eng.* 43(2004) 1129-1140.
13. A. Alhuthali and I. M. Low, *J. Mater. Sci.* 48 (2013) 4260–4273.
14. Pooja P. Adroja, S. B. Koradiya and P. H. Parsania, *Polym. Plast. Techno. and Engg,* 50 (2011) 52–58.
15. J. D. Thanki and P. H. Parsania, *World Scientific News,* 42 (2016)182-196.
16. Rizwan Y. Ghumara, Pooja P. Adroja and Parsotam H. Parsania, *Polym. Compos.* 37 (2016), 279–287.
17. J. V. Patel, J. P. Patel, R. D. Bhatt and P. H. Parsania, *J. Sci. Indus. Res.* 74 (2015), 577-581.
18. Jignesh V. Patel, Ritesh D. Bhatt and Parsotam H. Parsania, *J. Polym. Mater.* 31 (2014) 425-436.
19. A. B. Mathur and I. S. Bhardwaj,Testing and Evaluation of Plastics. Allied Publishers Pvt. Ltd., 2003.
20. A. I. Vogel, A. R. Tatchell, B. S. Funis, A. J. Hannaford and P. W. G. Smith, Vogel's Textbook of Practical Organic Chemistry 5th Ed., Addison Wesley Longman, UK, 1998, p 395.
21. B. Bhu**va a**nd P. Parsania, *J. Appl. Polym. Sci.* 118 (2010), 1469-1475.
2**2.** ASTM D 1980-87, Standard Method for Acid Value of Fatty Acids and Polymerized Fatty Acid, 1998.
23. T. J. Farmer, R. L. Castle, J. H. Clark and D. J. Macquarrie, *Int. J. Mol. Sci.* 16 (2015) 14912-14932.
24. D. A. Anderson and E. S. Freeman, *J. Polym. Sci.* 54 (1961) 253-260.
25. J. D. Thanki and P. H. Parsania, *J. Polym. Mater*. 33(2016) 305-317.
26. Jabal D. Thanki and P. H. Parsania *J Polym Mater* 33(2016) 101-109.
27. G. Pritchard and S. S. Speake, *Composites* 18 (1987) 227-232.
28. G. Camino, M. P. Luda, A. Y. Polishchuk, M. Revellino, R. Bla-NCOn, G. V. and Merle, *J. Mattinez, Compos. Sci. Technol.* 57(1997) 1469-1482.
29. L. R. Bao and A. F. Yee, *Polymer,* 43 (2002) 3987-3997.
30. A. Espert, F. Vilaplana and S. Karlsson, Composites Part A: *Appl. Sci. and Manuf.* **35** (2004) 1267-1276.

Received: 12-12-2017

Accepted: 07-05-2018